Interactions between the Chloride Anion and Aromatic Molecules: Infrared Spectra of the $Cl^-−C_6H_5CH_3$, $Cl^-−C_6H_5NH_2$ and $Cl^-−C_6H_5OH$ Complexes

Corinna Emmeluth, Berwyck L. J. Poad, Christopher D. Thompson, and Evan J. Bieske*

School of Chemistry, The University of Melbourne, Victoria, Australia 3010

Received: January 18, 2007; In Final Form: April 10, 2007

The $Cl^-−C_6H_5CH_3$·Ar, $Cl^-−C_6H_5NH_2$·Ar, and $Cl^-−C_6H_5OH$·Ar anion complexes are investigated using infrared photodissociation spectroscopy and ab initio calculations at the MP2/aug-cc-pVDZ level. The results indicate that for $Cl^-−C_6H_5NH_2$ and $Cl^-−C_6H_5OH$, the Cl^- anion is attached to the substituent group by a single near-linear hydrogen bond. For $Cl^-−C_6H_5CH_3$, the Cl^- is attached to an *ortho*-hydrogen atom on the aromatic ring and to a hydrogen atom on the methyl group by a weaker hydrogen bond. The principal spectroscopic consequence of the hydrogen-bonding interaction in the three complexes is a red-shift and intensity increase for the CH, NH, and OH stretching modes. Complexities in the infrared spectra in the region of the hydrogen-bonded XH stretch band are associated with Fermi resonances between the hydrogen-stretching vibrational modes and bending overtone and combination levels. There are notable correlations between the vibrational red-shift, the elongation of the H-bonded XH group, and the proton affinity of the aromatic molecule's conjugate base.

1. Introduction

This paper is concerned with the properties of the $Cl^-−C_6H_5CH_3$, $Cl^-−C_6H_5NH_2$, and $Cl^-−C_6H_5OH$ complexes as revealed through their infrared spectra in the hydrogen-stretching region and through ab initio calculations. Motivation for investigating these systems stems in part from the importance of interactions between simple ions such as Na^+, K^+, and Cl^- and the phenyl, alkyl, amino, and hydroxyl functional groups in different biological contexts, including ion transport in membrane channels. Prompted by this significance, Lisy and co-workers have investigated the interactions between simple metal cations ($M^+ = Na^+$, K^+) and aromatic molecules ($L = C_6H_6$, C_6H_5OH) through spectroscopic investigations of mixed $M^+−L_m−(H_2O)_n$ clusters.[1−5] It was found that whereas Na^+ ions are preferentially solvated by H_2O rather than by C_6H_6, the reverse is true for K^+. This situation is consistent with the preferential transfer of K^+ ions in certain membrane ion channels, where cation-π interactions play an important role. There have also been spectroscopic investigations of complexes involving benzene and other metal cations, including Al^+, V^+, Fe^+, Co^+, and N^+, in the 500−1500 cm^{-1} range using light generated by a free electron laser[6,7] and in the benzene CH stretch region (2700−3300 cm^{-1}) using light from an OPO.[7−9] These investigations confirm that the metal cation prefers to bind to the π cloud of the benzene ring.

Infrared spectroscopic investigations of the corresponding anion-aromatic complexes and clusters are scarcer. In one of the few previous studies, complexes of benzene with Cl^-, Br^-, and I^- were characterized using infrared photodissociation (IRPD) spectroscopy and through ab initio calculations.[10,11] The infrared spectra and quantum chemical calculations suggest that the complexes have planar structures in which the F^- anion is attached to the benzene by a single H-bond, whereas the larger halides (Cl^-, Br^-, I^-) are attached by twin H-bonds. In all cases, the configuration with the halide anion sitting atop the aromatic ring was found to be unstable, presumably due to repulsive interactions between the halide and the ring π cloud.

In the current study, we extend spectroscopic investigations to complexes consisting of a chloride anion attached to substituted benzene (SBz) molecules (toluene, aniline, phenol). We aim to identify the complexes' structures by following changes to the XH stretch vibrational frequencies of the SBz subunit caused by interaction with the chloride anion. Although there have been no previous infrared spectroscopic studies of halide−SBz complexes, thermochemical data (binding enthalpies and entropies) have been measured for several systems including $Cl^-−C_6H_5OH$, $Br^-−C_6H_5CH_3$, and $Br^-−C_6H_5NH_2$.[12−14] Additionally, Continetti and co-workers recently studied the dissociative photodetachment dynamics of the $I^-−C_6H_5NH_2$ complex using photoelectron−photofragment coincidence spectroscopy.[15] Density functional calculations accompanying the experimental work predicted that the anion complex has a structure in which the I^- anion is attached by a single hydrogen bond to the amine group.

2. Experimental and Theoretical Methods

2.1. Experimental Technique. The vibrational predissociation spectra of the Cl^-−SBz complexes were recorded in a low-energy guided ion beam apparatus.[16−18] The machine consists of a cluster ion source, a primary quadrupole mass filter, an octopole ion guide, a secondary quadrupole mass filter, and a microchannel plate detector. The complexes were synthesized in an electron beam crossed supersonic expansion of argon (6 bar) seeded with traces of CCl_4 (as a Cl^- precursor) and the SBz molecule of interest.

In all three cases, the Cl^-−SBz binding energy is likely to exceed the IR photon energy. For example, the binding enthalpy of $Cl^-−C_6H_5OH$ has been determined as 109.0 ± 8.4 kJ mol^{-1} (~9100 cm^{-1}).[12,13] Although to our knowledge, the binding enthalpies of $Cl^-−C_6H_5CH_3$ and $Cl^-−C_6H_5NH_2$ have not been reported, they almost certainly exceed those of $Br^-−C_6H_5CH_3$

* Corresponding author. E-mail: evanjb@unimelb.edu.au.

10.1021/jp070453r CCC: $37.00
Published on Web 05/27/2007

TABLE 1: Scaled Hydrogen Stretch Frequencies for $Cl^-{-}C_6H_5CH_3$, $Cl^-{-}C_6H_5NH_2$, and $Cl^-{-}C_6H_5OH$ (in cm^{-1}) with Infrared Intensities (km mol^{-1}) Given in Brackets[a]

$Cl^-{-}C_6H_5CH_3$		$Cl^-{-}C_6H_5NH_2$		$Cl^-{-}C_6H_5OH$	
mode	$\tilde{\nu}$	mode	$\tilde{\nu}$	mode	$\tilde{\nu}$
$\nu_{CH}^{s,al}$	2872 (75)	ν_{CH}	3005 (18)	ν_{OH}	2815 (2528)
$\nu_{CH}^{a,al}$	2957 (27)	ν_{CH}	3017 (4)	ν_{CH}	3022 (0.3)
$\nu_{CH}^{a,al/ar}$	2972 (74)	ν_{CH}	3025 (45)	ν_{CH}	3031 (39)
$\nu_{CH}^{s,al/ar}$	2978 (128)	ν_{CH}	3033 (204)	ν_{CH}	3048 (19)
ν_{CH}^{ar}	3009 (11)	ν_{NH}^{bound}	3047 (21)	ν_{CH}	3053 (43)
ν_{CH}^{ar}	3024 (13)	ν_{CH}	3073 (993)	ν_{CH}	3059 (29)
ν_{CH}^{ar}	3037 (39)	ν_{NH}^{free}	3473 (25)		
ν_{CH}^{ar}	3050 (43)				

[a] For $Cl^-{-}C_6H_5CH_3$, superscripts al and ar denote localization of the vibration on the aliphatic or aromatic CH groups, respectively. Asymmetric and symmetric vibrations are indicated by a and s, respectively.

and $Br^-{-}C_6H_5NH_2$ (36. ± 7.5 and 61.1 ± 7.5 kJ mol^{-1}, respectively[14]). So that we could monitor single IR photon absorption by cold complexes, we have probed argon-solvated species ($Cl^-{-}$SBz·Ar), monitoring Ar atom loss as a function of the infrared wavelength. The presence of a weakly attached Ar atom has been shown to have a minimal effect on the IR spectra of other anion complexes, the main consequence being a narrowing and slight shifting of the vibrational bands.[19,20]

The parent $Cl^-{-}$SBz·Ar clusters were mass-selected by a quadrupole mass filter, turned through 90° by a quadrupole bender, and injected into the octapole ion guide. Here, the clusters were irradiated with the counter-propagating output of a Nd:YAG-pumped OPO/OPA system (Continuum Mirage 3000). Resulting fragment ions were selected by a second quadrupole mass filter and sensed by a microchannel plate/scintillator/photomultiplier detector. Wavelength calibration was achieved by measuring the output from the first stage of the OPO and the 532 nm output from the Nd:YAG laser using a pulsed wavemeter (HighFinesse WS-7).

2.2. Theoretical Methods. Optimized geometries and vibrational frequencies for the $Cl^-{-}C_6H_5CH_3$, $Cl^-{-}C_6H_5NH_2$, and $Cl^-{-}C_6H_5OH$ complexes were calculated out at the Møller−Plesset second-order (MP2) level of theory, using Dunning's aug-cc-pVDZ basis set.[21] This method has previously been demonstrated as suitable for describing the structures and energetics of hydrogen-bonded complexes and clusters containing halide anions.[22,23] Calculations utilized the Gaussian 03 suite of programs.[24]

Simulated infrared spectra of the complexes were generated by scaling the calculated harmonic frequencies using a factor determined from the experimental and calculated harmonic hydrogen stretch frequencies of the SBz monomer. Experimental vibrational frequencies for toluene, aniline, and phenol were taken from refs 25−27. The resulting scaling factors were 0.9503 for toluene, 0.9583 and 0.9482 for the NH and CH stretches of aniline, and 0.9602 and 0.9514 for the OH and CH stretches of phenol. To generate the simulated IR spectra, the calculated transitions were convoluted by Gaussians having widths of 6 cm^{-1}. Scaled vibrational frequencies, intensities, and assignments for the three complexes are given in Table 1.

3. Results

3.1. $Cl^-{-}C_6H_5CH_3$. *Theoretical Results.* (a) Conformations and Dissociation Energy. A Cl^- anion can interact with a toluene molecule either through aliphatic or aromatic hydrogen atoms, making it an interesting system to study the competition between different types of hydrogen bonding. Different conformations of the $Cl^-{-}C_6H_5CH_3$ complex, corresponding to stationary points on the potential energy surface (PES), were calculated at the MP2/aug-cc-pVDZ level of theory and are shown in Figure 1.

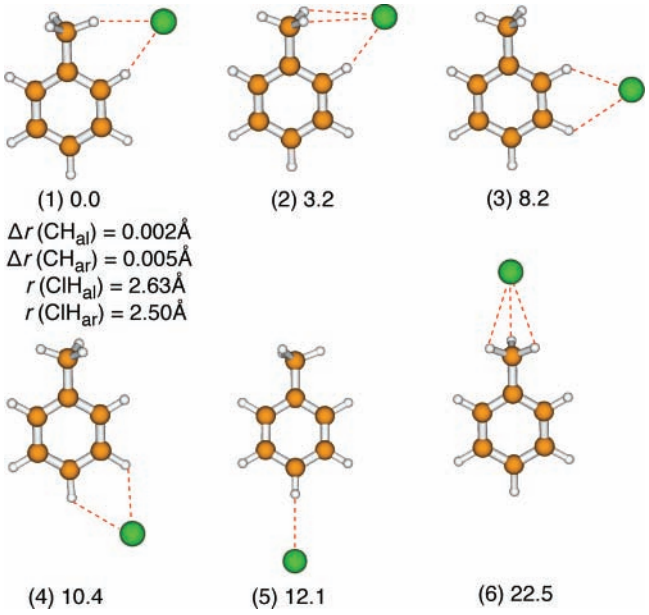

Figure 1. Low-energy conformations of $Cl^-{-}C_6H_5CH_3$ calculated at the MP2/aug-cc-pVDZ level. Relative energies (in kJ mol^{-1}) are given for each conformer.

The global minimum energy structure (structure 1) has the Cl^- attached to toluene by a double contact H-bond, through an *ortho*-hydrogen atom on the aromatic ring as well as a hydrogen atom on the methyl group. The dissociation energy corrected for vibrational zero-point energy (ZPE) is 45.4 kJ mol^{-1}; correction for basis set superposition error by the method of Boys and Bernardi[28] reduces the dissociation energy to 38.2 kJ mol^{-1}. Interestingly, it appears that the H-bond to the aromatic ring is stronger than the one to the methyl group. Evidence for this is that the distance between the *ortho*-H atom and the Cl^- ion is predicted to be 2.504 Å, whereas the distance between the methyl group H atom and the Cl^- ion is 2.628 Å. Furthermore, the H-bonded *ortho*-CH bond on the ring is lengthened by 0.5%, whereas the H-bonded CH on the methyl group is lengthened by only 0.2%. Double-contact H-bonds between halides and solvent molecules have also been observed for the $I^-{-}$HCOOH complex, in which both the OH and CH groups are attached to the I^-,[29] and in the $Cl^-{-}C_6H_6$, $Br^-{-}C_6H_6$, and $I^-{-}C_6H_6$ complexes where the halide anions are attached to two neighboring hydrogen atoms.[10]

There are several higher-energy stationary points for the $Cl^-{-}C_6H_5CH_3$ system; these are discussed in order of increasing energy. Starting with structure 1, rotation of the methyl group by 60° leads to structure 2, which is a first-order saddle point lying 3.2 kJ mol^{-1} higher in energy. Structure 3, in which the Cl^- anion is attached to the *ortho*- and *meta*-hydrogen atoms of the aromatic ring, is a stable minimum lying 8.2 kJ mol^{-1} above structure 1. For this structure, rotation of the methyl group by 60° changes the energy by <0.1 kJ mol^{-1}. Structure 4, in which the Cl^- is attached to the *meta*- and *para*-hydrogen atoms, is a stable geometry lying 10.4 kJ mol^{-1} above structure 1. Structure 5, in which the Cl^- is bound by a single H-bond to the *para*-hydrogen, lies 12.1 kJ mol^{-1} above structure 1. Finally, for structure 6, the Cl^- ion is attached to the methyl group by three equivalent hydrogen bonds. This configuration is a second-

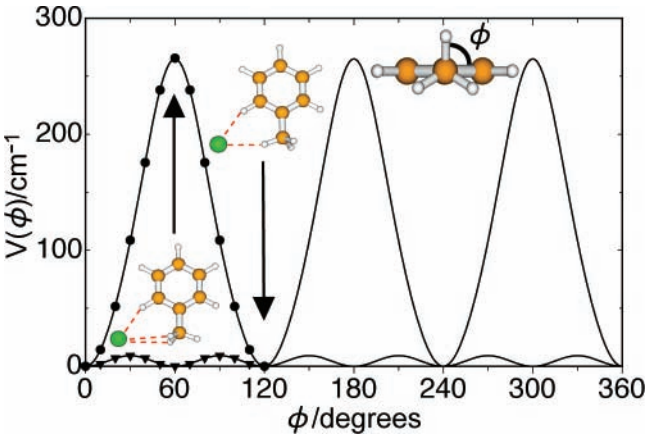

Figure 2. Torsional potential for the methyl group in the $Cl^-{-}C_6H_5CH_3$ complex (●) and bare toluene (▲) calculated at the MP2/aug-cc-pVDZ level.

order saddle point (with a doubly degenerate vibrational mode with imaginary frequency). The predicted infrared spectra associated with the different stable minima are discussed below in relation to the experimental spectrum.

(b) Rotation of the Methyl Group. One can anticipate that the methyl torsional potential for $Cl^-{-}C_6H_5CH_3$ will differ profoundly from that of $C_6H_5CH_3$ because the Cl^- anion is H-bonded to both the methyl group and the aromatic ring. To investigate the influence of the attached Cl^-, we calculated the methyl torsional potentials for $C_6H_5CH_3$ and $Cl^-{-}C_6H_5CH_3$ at the MP2/aug-cc-pVDZ level in relaxed scans along the methyl torsional angle ϕ. The resulting torsional potential energy curves are shown in Figure 2. The potential energy curve for the toluene monomer exhibits a very small barrier for methyl internal rotation (13 cm^{-1}) and a parallel minimum energy configuration ($\phi = 0°$). Experimentally, toluene is found to have a 4.9 cm^{-1} barrier for internal rotation and a perpendicular minimum energy configuration ($\phi = 90°$).[30,31] As the torsional potential curve for $C_6H_5CH_3$ is extremely shallow and depends on rather subtle interactions, it is perhaps not surprising that the MP2/aug-cc-pVDZ calculations fail to predict the correct configuration. As expected, the torsional potential is significantly modified for $Cl^-{-}C_6H_5CH_3$ because of the dual H-bonds between Cl^- and H atoms on the methyl group and the ring; the torsional barrier increases to 266 cm^{-1} and the hindering potential exhibits 3 equivalent minima.

Experimental Results. The photodissociation IR spectrum of $Cl^-{-}C_6H_5CH_3{\cdot}Ar$ is displayed in Figure 3, along with the simulated spectra based on the scaled MP2/aug-cc-pVDZ vibrational frequencies and intensities for the four stable structures (structures 1 and 3−5 in Figure 1). The experimental spectrum is dominated by an intense broad feature centered near 2970 cm^{-1}, with weaker features occurring above 3000 cm^{-1} and below 2940 cm^{-1}. The $Cl^-{-}C_6H_5CH_3{\cdot}Ar$ spectrum differs significantly from the spectrum of the jet-cooled $C_6H_5CH_3$ monomer recorded by Fuji et al.[32] For $Cl^-{-}C_6H_5CH_3$ the CH stretch band structure spans a range (2850−3075 cm^{-1}) that is slightly lower in frequency than for the toluene monomer (2870−3100 cm^{-1}). Most noticeably, the dominant feature in the $Cl^-{-}C_6H_5CH_3{\cdot}Ar$ spectrum occurs around 65 cm^{-1} lower in energy than the dominant peak in the toluene spectrum (3035 cm^{-1}). The differences are presumably due to the influence of the ionic H-bonds on the CH stretch vibrational frequencies.

Evidence for the structure of $Cl^-{-}C_6H_5CH_3$ can be obtained by comparing the experimental and simulated infrared spectra in the CH stretch region. Inspection of Figure 3 shows that the

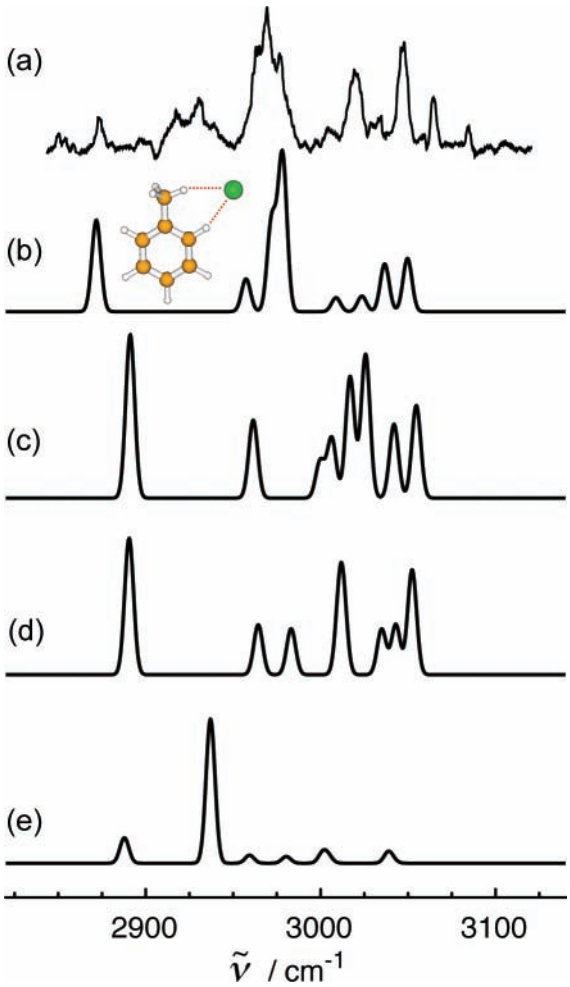

Figure 3. (a) Experimental infrared spectrum of $Cl^-{-}C_6H_5CH_3{\cdot}Ar$, and (b−e) simulated spectra based on calculations at the MP2/aug-cc-pVDZ level of theory for the 4 local minima shown in Figure 1. Trace (b) corresponds to the global minimum (structure 1), (c) to structure 3, (d) to structure 4, and (e) to structure 5. Scaled vibrational frequencies, intensities, and assignments for the global minimum structure are given in Table 1.

$Cl^-{-}C_6H_5CH_3$ experimental spectrum bears a reasonable resemblance to the simulated spectrum associated with global minimum energy structure (structure 1 in Figure 1). In particular, the broad, intense central feature is reproduced in the simulated spectrum by a band that is the superposition of two transitions associated with the symmetric and asymmetric stretch vibration of the two H-bonded hydrogen atoms. The weaker features above 3000 cm^{-1} correspond to aromatic CH stretch vibrational modes, whereas features below 2940 cm^{-1} are attributable to the methyl CH stretch vibrational modes.

Aside from the broad central feature, it is difficult to make a direct correspondence between the peaks in the experimental and simulated spectrum for structure 1; the experimental spectrum contains 8−10 distinct bands, whereas the simulated spectrum exhibits eight bands. Additional bands may arise from Fermi resonances between the IR bright CH stretch states and near resonance overtone and combination levels associated with the in-plane bend modes; such resonances also play a significant role in the spectral structure of the toluene and benzene monomers.[32,33]

The simulated spectra of the higher-energy $Cl^-{-}C_6H_5CH_3{\cdot}Ar$ structures (structures 3−5 in Figure 3) show less resemblance to the experimental spectrum; in each case, the intense central feature is absent from the simulated spectrum. Structures 3 and

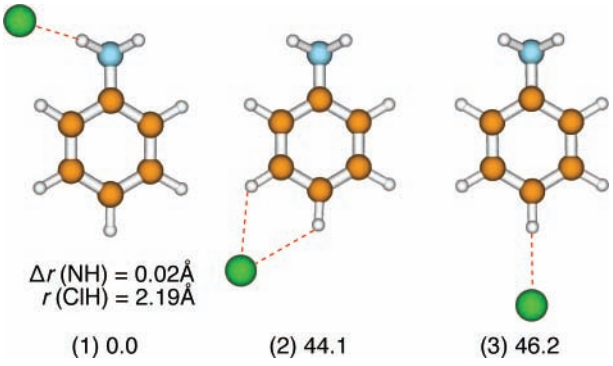

Figure 4. Stable conformers of $Cl^-{-}C_6H_5NH_2$. Relative energies (in kJ mol^{-1}) are given for each conformer.

4 would be expected to show a prominent methyl CH stretch band at 2885 cm^{-1}, whereas structure 5 should be dominated by a band at 2935 cm^{-1} associated with stretching vibration of the H-bonded *para*-hydrogen atom. Although most of the ions probed experimentally probably have structure 1, it is possible that minor fractions of the population have the higher-energy structures 3−5. Therefore, it is conceivable that additional peaks in the experimental spectrum are associated with these less stable forms.

3.2. $Cl^-{-}C_6H_5NH_2$. *Theoretical Results.* At the MP2/aug-cc-pVDZ level, $Cl^-{-}C_6H_5NH_2$ is found to have the three stable minima shown in Figure 4. The lowest-energy structure features a near-linear H-bond between the Cl^- and one amine hydrogen (structure 1; bond angle of 173.2°), similar to the calculated structure of the $I^-{-}C_6H_5NH_2$ complex.[15] This conformer has a ZPE corrected dissociation energy $D_0 = 75.6$ kJ mol^{-1}, with BSSE correction reducing this to 68.5 kJ mol^{-1}. Although the association enthalpy of $Cl^-{-}C_6H_5NH_2$ has not been measured, the calculated D_0 is bracketed by the experimental association enthalpies of $F^-{-}C_6H_5NH_2$ (131.0 ± 8.4 kJ/mol[34]) and $Br^-{-}C_6H_5NH_2$ (61.1 ± 7.5 kJ mol^{-1} [14]). There are two higher-energy structures. In the first (structure 2), which lies higher in energy than the global minimum by 44.1 kJ mol^{-1}, the Cl^- is H-bonded to the *meta*- and *para*-hydrogens. In the second (structure 3), which lies an additional 2.1 kJ mol^{-1} higher in energy, the Cl^- is bound linearly to the *para*-hydrogen of the aromatic ring. Barriers for interconversion between structures 2 and 1 and between structures 3 and 2 are 0.5 kJ mol^{-1} and 2.1 kJ mol^{-1}, respectively. Because of the much greater stability of structure 1 and low interconversion barriers it is unlikely that structures 2 or 3 would be formed in the ion source.

The calculated barrier for the umbrella inversion of the amine group in $Cl^-{-}C_6H_5NH_2$ is 2.8 kJ mol^{-1}, compared to 6.0 kJ mol^{-1} for bare aniline (experiment: 6.3 kJ mol^{-1} [35,36]). The rather low barrier for umbrella inversion in the complex is unexpected given that MP2/aug-cc-pVTZ calculations predicted a larger inversion barrier for $Cl^-{-}NH_3$ compared to bare NH_3.[37] A possible explanation for the low inversion barrier in $Cl^-{-}C_6H_5NH_2$ is that the Cl^--π cloud repulsion is minimized for the planar configuration and the opportunity for a weak secondary H-bond between the *ortho*-CH group and the Cl^- is maximized.

The barrier for transferring the Cl^- from one H to the other on the NH_2 group is 17.2 kJ mol^{-1}, considerably higher than the 6.4 kJ mol^{-1} barrier for $Cl^-{-}NH_3$.[37] This may be a consequence of the stronger intermolecular H-bond in the $Cl^-{-}C_6H_5NH_2$ complex compared to $Cl^-{-}NH_3$.

Experimental Results. The IR spectrum of the jet-cooled aniline monomer contains a series of aromatic CH stretch bands in the 3000−3120 cm^{-1} region and symmetric and asymmetric NH_2 stretch bands at 3423 and 3509 cm^{-1}, respectively.[38] The aromatic CH stretch bands and the NH_2 bands are of comparable intensity. In contrast, the IR spectrum for $Cl^-{-}C_6H_5NH_2$, shown in Figure 5, is dominated by a strong peak at 2920 cm^{-1} that can be assigned to a red-shifted H-bonded NH stretch mode for structure 1 shown in Figure 4. The free NH stretch band appears as a small but unmistakable peak at 3475 cm^{-1}, approximately midway between the symmetric and asymmetric NH stretch bands of the $C_6H_5NH_2$ monomer (indicated by arrows in Figure 5). The red-shift for the H-bonded NH stretch band for $Cl^-{-}C_6H_5NH_2$ with respect to the average of the symmetric and asymmetric NH_2 stretch bands of the $C_6H_5NH_2$ monomer (3466 cm^{-1}) is 546 cm^{-1}.

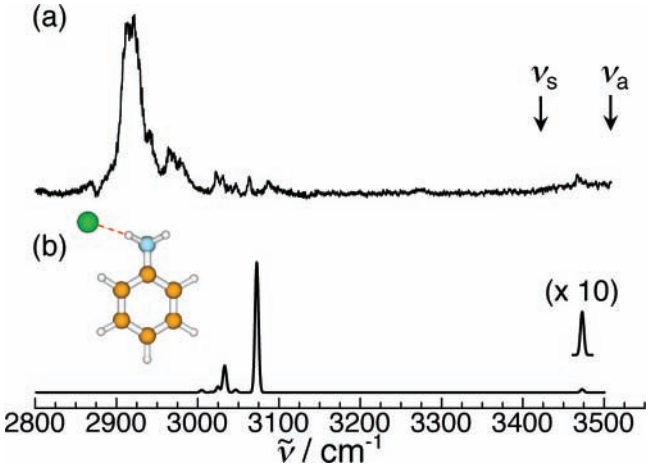

Figure 5. (a) Experimental infrared spectrum of $Cl^-{-}C_6H_5NH_2{\cdot}Ar$, and (b) simulated spectrum based on calculations at the MP2/aug-cc-pVDZ level. Arrows indicate symmetric and asymmetric NH_2 stretch bands for $C_6H_5NH_2$.[26] Scaled vibrational frequencies, intensities, and assignments are given in Table 1.

Several much weaker bands appear in the aromatic CH stretch region (3000−3100 cm^{-1}). The feature centered at 2970 cm^{-1} does not correspond to any band in the simulated spectrum and may represent a combination or overtone band deriving intensity through Fermi resonance with the strongly red-shifted NH stretch mode.

Comparison of the experimental spectrum and the simulated spectrum for structure 1 suggests that the scaled harmonic frequency for the H-bonded NH stretch mode (3073 cm^{-1}) overestimates the experimental value (2920 cm^{-1}). Presumably, this is because the scaling does not adequately account for the extreme anharmonicty of the H-bonded NH stretch coordinate. This issue is addressed more thoroughly in the Discussion section.

3.3. $Cl^-{-}C_6H_5OH$. *Theoretical Results.* The MP2/aug-cc-pVDZ calculations suggest that Cl^- prefers to bind to the hydroxy group of the C_6H_5OH molecule (structure 1, Figure 6). This structure has a ZPE-corrected dissociation energy of $D_0 = 107.1$ kJ mol^{-1}, with BSSE correction reducing this to 99.3 kJ mol^{-1}. The calculated value compares reasonably well with the measured association enthalpy (109.0 ± 8.4 kJ mol^{-1} [13]). The OH bond is elongated from 0.968 Å for bare phenol to 1.013 Å for the complex. This significant elongation, which can be viewed as reflecting incipient proton transfer to the Cl^- anion, is also reflected in a large red-shift of 841 cm^{-1} in the scaled harmonic stretch frequency. The $Cl^-{\cdots}H$ intermolecular bond length (1.969 Å) is significantly shorter than that for $Cl^-{-}C_6H_5CH_3$ (2.628 and 2.504 Å) and $Cl^-{-}C_6H_5$-NH_2 (2.166 Å).

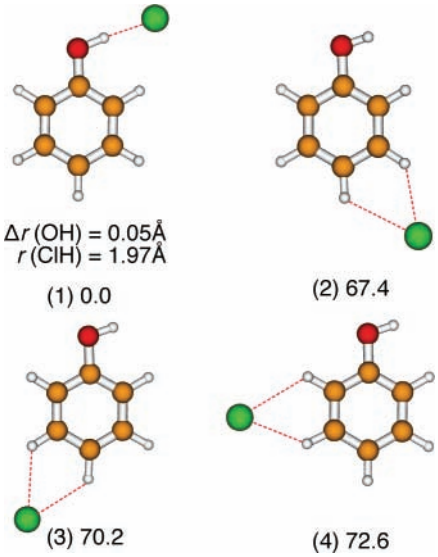

Figure 6. Calculated minima (MP2/aug-cc-pVDZ) for $Cl^-{-}C_6H_5OH$. Relative energies (in kJ mol^{-1}) are given for each conformer.

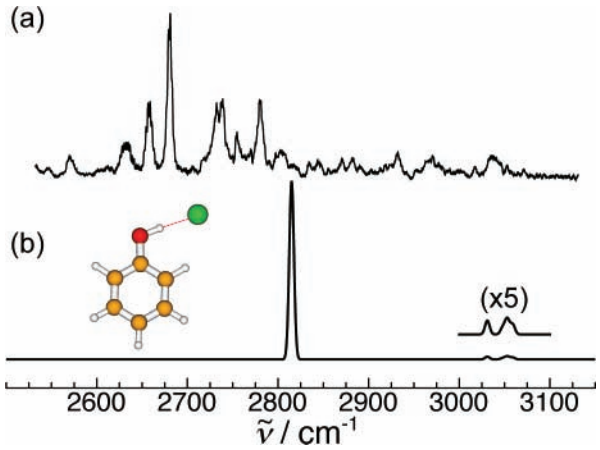

Figure 7. (a) Experimental infrared spectrum of $Cl^-{-}C_6H_5OH{\cdot}Ar$, and (b) a simulated spectrum based on calculations at the MP2/aug-cc-pVDZ level of theory. Scaled vibrational frequencies, intensities, and assignments are given in Table 1.

There are several higher-energy structures in which the anion is attached to two hydrogen atoms on the aromatic ring (structure 2−4, Figure 6). In all cases, both the hydroxy group and the anion lie in the plane of the ring, so that the complexes have C_s symmetry. The barrier to interconversion between structures 2 and 1 is only 0.2 kJ mol^{-1}, that between Structures 3 and 2 is 1.4 kJ mol^{-1}, and that between structures 4 and 3 is 0.5 kJ mol^{-1}. Given the relative stability of structure 1 and low barriers for interconversion, it is unlikely that structures 2−4 were formed in the ion source.

Experimental Results. The IR spectrum of the jet-cooled phenol monomer recorded by Yamada et al. contains an OH stretch band at 3657 cm^{-1} and a series of aromatic CH stretch bands in the 3020−3120 cm^{-1} range.[27] One can anticipate that formation of a strong H-bond between the Cl^- and the OH group on the phenol will lead to a large red-shift and intensity increase for the OH stretch band, whereas the CH stretch bands should be largely unaffected. Indeed, the predicted spectrum for the H-bonded form of $Cl^-{-}C_6H_5OH$ (structure 1 in Figure 6) is dominated by an intense red-shifted band at 2815 cm^{-1} associated with the OH stretch vibration, with weaker CH stretch bands occurring in the 3000−3100 cm^{-1} region (Figure 7). As predicted, several weak bands occur in the 3000−3100 cm^{-1} aromatic CH stretch region of the experimental spectrum. However, rather than displaying a single OH stretch band, the experimental spectrum (Figure 7) exhibits a series of strong bands (at 2658, 2680, 2732, 2738, and 2780 cm^{-1}) in a region somewhat below where the calculations predict the H-bonded OH stretch should occur. These features are probably attributable to the OH stretch mode and neighouring combination and overtone levels gaining IR intensity through Fermi resonance. If this is the case, the zero-order frequency for the H-bonded OH stretch mode can be estimated from the center of gravity of the bands in the 2550−2850 cm^{-1} range. The resulting zero-order OH stretch frequency (2725 cm^{-1}) corresponds to a red-shift of ∼930 cm^{-1} with respect to the OH stretch band of the C_6H_5OH monomer (3657 cm^{-1}). As in the case of $Cl^-{-}C_6H_5NH_2$, it seems that the scaled harmonic frequency for the H-bonded OH stretch mode (2815 cm^{-1}) overestimates the experimental value, presumably because the frequency scaling does not adequately account for the extreme anharmonicty in the H-bonded XH stretch coordinate. This issue is addressed below.

4. Discussion

The calculations and infrared spectra described in the preceding section suggest that the $Cl^-{-}C_6H_5CH_3$, $Cl^-{-}C_6H_5NH_2$, and $Cl^-{-}C_6H_5OH$ complexes all possess structures in which the Cl^- is hydrogen bonded to a single hydrogen atom on the substituent group. In the case of $Cl^-{-}C_6H_5CH_3$, there is also a second, stronger H-bond with the *ortho*-hydrogen atom on the aromatic ring. Although for all three complexes, higher-lying isomers in which the Cl^- anion is H-bonded to one or two hydrogen atoms on the phenyl ring are predicted, the barriers for conversion to the lowest-energy form are generally found to be small. For the lowest-energy form of all three $Cl^-{-}$SBz complexes, the principal spectroscopic consequence of the hydrogen-bonding interaction is a red-shift and intensity increase for the CH, NH, and OH stretching modes. Unfortunately, straightforward comparisons between the experimental and simulated spectra are complicated by Fermi resonances between the H-bonded XH stretch mode and bending overtones and combinations, particularly for $Cl^-{-}C_6H_5CH_3$ and $Cl^-{-}C_6H_5OH$. Nevertheless, in all three cases, there is clearly a systematic red-shift and intensity increase in vibrational modes associated with the H-bonded XH groups.

The $Cl^-{-}$SBz complexes can be considered as intermediates for the proton-transfer reaction

$$Cl^- + HA \rightarrow HCl + A^-$$

Because the proton affinity (PA) of Cl^- (14.46 eV[39]) is less than the PAs of $C_6H_5CH_2^-$, $C_6H_5NH^-$, and $C_6H_5O^-$ (16.45, 15.89, and 15.16 eV, respectively[39]), the complexes consist essentially of a Cl^- anion attached to a perturbed SBz molecule. Nevertheless, there is a degree of proton transfer from the SBz to the chloride anion, the extent of which is determined by the difference between the proton affinities (ΔPA) of the Cl^- and the A^- base. The degree of proton transfer is reflected in the magnitudes of the vibrational red-shift for the H-bonded XH group and elongation of the H-bonded XH bond.[40] The experimental red-shifts follow the expected trend, with $Cl^-{-}C_6H_5CH_3$ (large ΔPA) exhibiting the smallest red-shift and $Cl^-{-}C_6H_5OH$ (small ΔPA) the largest.

The experimental frequencies for the H-bonded NH and OH stretch vibrations of $Cl^-{-}C_6H_5NH_2$ and $Cl^-{-}C_6H_5OH$ are somewhat lower than the scaled calculated harmonic frequencies

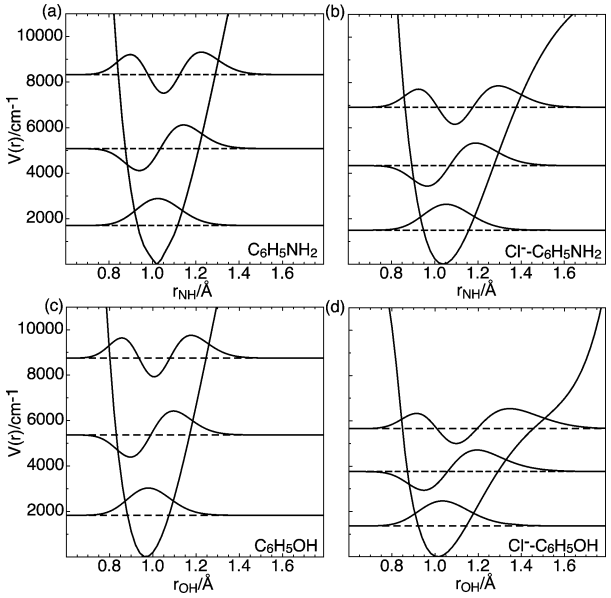

Figure 8. One-dimensional NH/OH stretch potential energy curves (calculated at the MP2/aug-cc-pVDZ level) for (a) $C_6H_5NH_2$, (b) Cl^-—$C_6H_5NH_2$, (c) C_6H_5OH, and (d) Cl^-—C_6H_5OH. In each case, the lowest three energy levels and associated wave functions are shown.

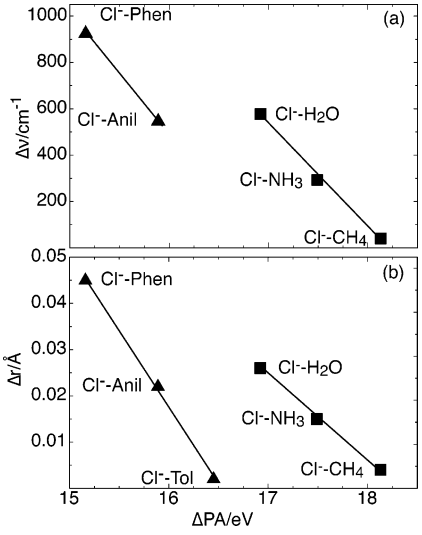

Figure 9. Correlation between (a) experimental vibrational redshift and (b) calculated bond elongation (at MP2/aug-cc-pVDZ level) and the difference in proton affinities (ΔPA) of Cl^- and conjugate base A^-. Filled triangles (▲) represent Cl^-—SBz complexes, whereas filled squares (■) represent complexes of Cl^- and second-row hydride molecules.

(see Figures 5 and 7). A likely source of the discrepancy is anharmonicity in the H-bonded XH stretch coordinate not fully accounted for by frequency scaling. To investigate this possibility, we calculated one-dimensional potential energy curves (at the MP2/aug-cc-pVDZ level) for the H-bonded XH stretch motion (with remaining coordinates fixed). Plots for both the free SBz molecule and the corresponding Cl^-—SBz complex appear alongside one another in Figure 8, highlighting the influence of the attached Cl^- ion. The distortion of the potential energy curves for Cl^-—$C_6H_5NH_2$ and Cl^-—C_6H_5OH is quite evident, illustrating the marked delocalization of the shared proton.

Frequencies for the hydrogen stretch vibrations associated with the one-dimensional potential curves were calculated using Level 7.4,[41] assuming that the vibration involved only motion of the H-bonded hydrogen atom. The effective mass of the oscillator was assumed to be 1 amu. The first three vibrational levels are superimposed on the potential curves in Figure 8. For Cl^-—$C_6H_5NH_2$, the NH stretch transition is calculated to lie at 2845 cm^{-1}, comparing favorably with the experimental value (2920 cm^{-1}), and certainly better than the scaled harmonic prediction, which overestimates the experimental frequency by 150 cm^{-1}. For Cl^-—C_6H_5OH, the OH stretch frequency is calculated to lie at 2400 cm^{-1}, around 415 cm^{-1} below the scaled harmonic frequency, and indeed below the series of bands apparent in the experimental spectrum between 2600 and 2800 cm^{-1}. This raises the possibility that the OH stretch band occurs below 2550 cm^{-1}, beyond the wavelength range of the OPO used in this work. However, it is also feasible that the reduced mass used in the 1D vibrational frequency calculations is slightly too high, leading to an overestimation of the stretching frequency.

One might expect that there should be similarities between the Cl^-—SBz complexes (Cl^-—$C_6H_5CH_3$, Cl^-—$C_6H_5NH_2$, Cl^-—C_6H_5OH) and complexes of Cl^- and the second-row hydride molecules (Cl^-—CH_4, Cl^-—NH_3, and Cl^-—H_2O), which have also been studied using infrared spectroscopy and through ab initio calculations.[37,42,43] In effect, the two sets can be distinguished as CH_3, NH_2, or OH functionalities associated with either an H or C_6H_5 subgroup. The extent of proton transfer to the Cl^- anion can be expected to be larger for the SBz molecules, because the PAs for $C_6H_5CH_2^-$, $C_6H_5NH^-$, and $C_6H_5O^-$ (16.45, 15.89, and 15.16 eV) are lower than those of CH_3^-, NH_2^-, and OH^- (18.13, 17.49, and 16.92 eV[44]). This is reflected in the magnitudes of the vibrational red-shifts and the elongation of the XH bond (calculated at the MP2/aug-cc-pVDZ level), both of which are plotted against ΔPA in Figure 9. Note that for Cl^-—$C_6H_5CH_3$, it is difficult to ascertain the magnitude of the red-shift because of the complexity of the spectrum and because both the aromatic and aliphatic CH stretch modes are affected by H-bonding. It is obvious from Figure 9 that the Cl^-—SBz complexes are associated with larger red-shifts and XH bond elongations than the complexes containing the corresponding second-row hydride molecule. For both sets of complexes, there is a near-linear correlation between ΔPA and the vibrational red-shift and the XH bond elongation.

Last, we consider the effect of the attached Ar atom. Although in each case the experimental spectrum does not provide direct information on the position of the Ar atom, presumably because the Ar···Cl^- bond (D_0 = 523 cm^{-1}; ref[45]) is comparable in strength with Ar···aromatic bonds (for example, $D_0 = 314 \pm 7$ cm^{-1} for C_6H_6·Ar; ref[46]), the Ar atom is positioned so as to maximize the interaction with both the Cl^- and the SBz subunit. For Cl^-—C_6H_6·Ar, Albertí et al. found that the most favorable location for the Ar atom is midway between the benzene ring and the Cl^-, so that it is stabilized by interactions with both the anion and the Bz molecule.[47] The situation is probably similar for the Cl^-—SBz complexes.

5. Summary

Infrared spectra have been recorded for Cl^-—$C_6H_5CH_3$·Ar, Cl^-—$C_6H_5NH_2$·Ar, and Cl^-—C_6H_5OH·Ar using vibrational predissociation spectroscopy. Accompanying ab initio calculations suggest that the lowest-energy conformers for Cl^-—$C_6H_5NH_2$ and Cl^-—C_6H_5OH have the Cl^- bound to a single hydrogen atom of the substituent group. In the case of Cl^-—$C_6H_5CH_3$, the Cl^- is hydrogen bonded to an *ortho*-hydrogen atom on the ring and to a hydrogen atom on the methyl group. Complexities in the infrared spectra are postulated to arise from Fermi resonances between the H-bonded XH stretch and overtone and

combination levels. There is a clear correlation between the proton affinity of the aromatic molecule's conjugate base and both the vibrational red-shift and the elongation of the H-bonded XH group ($Cl^--C_6H_5CH_3 < Cl^--C_6H_5NH_2 < Cl^--C_6H_5OH$).

Acknowledgment. The authors acknowledge support from the Australian Research Council, the University of Melbourne, and the National Facility of the Australian Partnership for Advanced Computing. This work was supported by a fellowship within the Postdoc-Programme of the German Academic Exchange Service (DAAD).

References and Notes

(1) Cabarcos, O. M.; Weinheimer, C. J.; Lisy, J. M. *J. Chem. Phys.* **1998**, *108*, 5151−5154.
(2) Cabarcos, O.; Weinheimer, C.; Lisy, J. *J. Chem. Phys.* **1999**, *110*, 8429−8435.
(3) Patwari, G. N.; Lisy, J. M. *J. Chem. Phys.* **2003**, *118*, 8555−8558.
(4) Patwari, G. N.; Lisy, J. M. *J. Phys. Chem. A* **2003**, *107*, 9495−9498.
(5) Vaden, T. D.; Lisy, J. M. *J. Chem. Phys.* **2004**, *120*, 721−730.
(6) Jaeger, T. D.; van Heijnsbergen, D.; Klippenstein, S. J.; von Helden, G.; Meijer, G.; Duncan, M. A. *J. Am. Chem. Soc.* **2004**, *126*, 10981−10991.
(7) Jaeger, T.; Pillai, E.; Duncan, M. *J. Phys. Chem. A* **2004**, *108*, 6605−6610.
(8) Jaeger, T. D.; Duncan, M. A. *J. Phys. Chem. A* **2005**, *109*, 3311−3317.
(9) Jaeger, T. D.; Duncan, M. A. *Int. J. Mass Spectrom.* **2005**, *241*, 165−171.
(10) Loh, Z. M.; Wilson, R. L.; Wild, D. A.; Bieske, E. J.; Zehnacker, A. *J. Chem. Phys.* **2003**, *119*, 9559−9567.
(11) Thompson, C.; Poad, B. L. J.; Emmeluth, C.; Bieske, E. *Chem. Phys. Lett.* **2006**, *428*, 18−22.
(12) Cumming, J.; French, M.; Kebarle, P. *J. Am. Chem. Soc.* **1977**, *99*, 6999−7003.
(13) French, M. A.; Ikuta, S.; Kebarle, P. *Can. J. Chem.* **1982**, *60*, 1907−18.
(14) Paul, G.; Kebarle, P. *J. Am. Chem. Soc.* **1991**, *113*, 1148−1154.
(15) Bowen, M. S.; Becucci, M.; Continetti, R. E. *J. Chem. Phys.* **2006**, *125*, 133309.
(16) Weiser, P. S.; Wild, D. A.; Bieske, E. J. *J. Chem. Phys.* **1999**, *110*, 9443−9449.
(17) Bieske, E. J. *Chem. Soc. Rev.* **2003**, *32*, 231−7.
(18) Wild, D. A.; Bieske, E. J. *Int. Rev. Phys. Chem.* **2003**, *22*, 129−151.
(19) Ayotte, P.; Weddle, G. H.; Kim, J.; Johnson, M. A. *J. Am. Chem. Soc.* **1998**, *120*, 12361−12362.
(20) Wild, D.; Loh, Z.; Wilson, R.; Bieske, E. *Chem. Phys. Lett.* **2003**, *369*, 684−690.
(21) Woon, D.; Dunning, T. *J. Chem. Phys.* **1993**, *98*, 1358−1371.
(22) Woon, D. E.; Duninng, T. H., Jr. *J. Chem. Phys.* **1994**, *100*, 2975.
(23) Xantheas, S. S. *J. Phys. Chem.* **1996**, *100*, 9703−9713.
(24) Frisch, M. J.; Trucks, G. W.; Schlegel, H. B.; et. al *Gaussian 03*, Revision D.01; Gaussian, Inc.: Pittsburgh, PA, 2005.
(25) Hickman, C. G.; Gascooke, J. R.; Lawrance, W. D. *J. Chem. Phys.* **1996**, *104*, 4887−4901.
(26) Nakanaga, T.; Ito, F.; Miyawaki, J.; Sugawara, K.; Takeo, H. *Chem. Phys. Lett.* **1996**, *261*, 414−420.
(27) Yamada, Y.; Ebata, T.; Kayano, M.; Mikami, N. *J. Chem. Phys.* **2004**, *120*, 7400−7409.
(28) Boys, S. F.; Bernardi, F. *Mol. Phys.* **1970**, *19*, 553.
(29) Robertson, W. H.; Kelley, J. A.; Johnson, M. A. *J. Chem. Phys.* **2000**, *113*, 7879−7884.
(30) Kreiner, W. A.; Rudolph, H. D.; Tan, B. T. *J. Mol. Spectrosc.* **1973**, *48*, 86.
(31) Borst, D. R.; Pratt, D. W. *J. Chem. Phys.* **2000**, *113*, 3658−3669.
(32) Fujii, A.; Fujimaki, E.; Ebata, T.; Mikami, N. *J. Chem. Phys.* **2000**, *112*, 6275−6284.
(33) Page, R. H.; Shen, Y.; Lee, Y. *J. Chem. Phys.* **1988**, *88*, 4621−4636.
(34) Larson, J.; McMahon, T. *J. Am. Chem. Soc.* **1983**, *105*, 2944.
(35) Larsen, N. W.; Hansen, E. L.; Nicolaisen, F. M. *Chem. Phys. Lett.* **1976**, *43*, 584−586.
(36) Kydd, R. A.; Krueger, P. J. *Chem. Phys. Lett.* **1977**, *49*, 539−543.
(37) Weiser, P. S.; Wild, D. A.; Wolynec, P. P.; Bieske, E. J. *J. Phys. Chem. A* **2000**, *104*, 2562−2566.
(38) Yamada, Y.; Okano, J.; Mikami, N.; Ebata, T. *J. Chem. Phys.* **2005**, *123*, 124316.
(39) Bartmess, J. "Negative Ion Energetics Data. In *NIST Chemistry WebBook*; NIST Standard Reference Database Number 69; Linstrom, P. J., Mallard, W. G., Eds.; National Institute of Standards and Technology: Gaithersburg, MD, 2005; http://webbook.nist.gov.
(40) Meot-Ner, M. *Chem. Rev.* **2005**, *105*, 213−284.
(41) Le Roy, R. *LEVEL 7.4: A Computer Program for Solving the Radial Schrödinger Equation for Bound and Quasibound Levels*; University of Waterloo: Waterloo, ON, 2001.
(42) Wild, D.; Loh, Z.; Wolynec, P.; Weiser, P.; Bieske, E. *Chem. Phys. Lett.* **2000**, *332*, 531−537.
(43) Kelley, J.; Weber, J.; Lisle, K.; Robertson, W.; Ayotte, P.; Johnson, M. *Chem. Phys. Lett.* **2000**, *327*, 1−6.
(44) Meot-Ner (Mautner), M.; Lias, S. Binding Energies Between Ions and Molecules, and the Thermochemistry of Cluster Ions. In *NIST Chemistry WebBook*; NIST Standard Reference Database Number 69; Linstrom, P. J., Mallard, W. G.; National Institute of Standards and Technology: Gaithersburg, MD, 2005; http://webbook.nist.gov.
(45) Lenzer, T.; Yourshaw, I.; Furlanetto, M. R.; Reiser, G.; Neumark, D. M. *J. Chem. Phys.* **1999**, *110*, 9578−9586.
(46) Sampson, R. K.; Lawrance, W. D. *Aust. J. Chem.* **2003**, *56*, 275−277.
(47) Albertí, M.; Castro, A.; Laganà, A.; Moix, M.; Pirani, F.; Cappelletti, D. *Eur. Phys. J. D* **2006**, *38*, 185−191.